Low speed operation improvement of MRAS sensorless vector control induction motor drive using neural network flux observers

Shady M Gadoue
School of Electrical Electronic and Computer Engineering
University of Newcastle upon Tyne
Newcastle upon Tyne
NE1 7RU, UK
Shady.Gadoue@ncl.ac.uk

Damian Giaouris
School of Electrical Electronic and Computer Engineering
University of Newcastle upon Tyne
Newcastle upon Tyne
NE1 7RU, UK
Damian.Giaouris@ncl.ac.uk

John W Finch
School of Electrical Electronic and Computer Engineering
University of Newcastle upon Tyne
Newcastle upon Tyne
NE1 7RU, UK
J.W.Finch@ncl.ac.uk

Abstract – **This paper presents a novel neural network-based flux observer to solve the low speed problems associated with a model reference adaptive speed estimation scheme which is based on rotor flux. A multilayer feedforward artificial neural network is proposed for rotor flux estimation which is more robust to noise and stator resistance variation and does not have dc-drift problems which are usually associated with these adaptive schemes. A comparison between the performance of the neural network based strategy and conventional scheme is carried out using a validated simulation of an indirect vector controlled induction motor drive working at a low speed.**

I. INTRODUCTION

During the last decade there has been considerable interest in sensorless control of AC motors, particularly, induction motors. Sensorless vector controlled induction motor drives are being vigorously developed for high performance industrial drive systems. Elimination of the speed sensor reduces the drive cost and size, and should increase the system reliability and robustness, and reduce the noise sensitivity and maintenance requirements. On the other hand, stability in the low and zero speed operation range, parameter sensitivity and high computational effort can be the main drawbacks of sensorless control [1]. Sensorless drives have been successfully applied for medium and high speed operation, but low and zero speed operation is still a critical problem. Much recent research effort is focused in this area [1, 2].

Estimation techniques in sensorless induction motor drives can be generally grouped into rotor saliency and terminal quantities-based techniques. Terminal quantities-based estimation strategies can be subdivided into Model Reference Adaptive Schemes (MRAS), observer-based schemes and Artificial Intelligence (AI) based methods. MRAS schemes are the most common strategies employed due to their relative simplicity and low computational effort [2].

Among various MRAS schemes, Rotor Flux (RF), back EMF and reactive power techniques are the most popular strategies which have received a lot of attention. Although back EMF based techniques avoid pure integration, they may have stability problems at low stator frequency and show low noise immunity. The reactive power method is characterized by its robustness against stator resistance variation but suffers from instability [3].

Rotor flux schemes suffer from parameter sensitivity, inaccuracy at low speed due to poor signal to noise ratio, dominant stator resistance drop and increased nonlinearity, deterioration of estimation at zero-speed operation and flux pure integration problems which may cause dc drift and initial condition problems [1, 3, 4]. To avoid problems associated with pure integration, a lot of strategies have been proposed for offset and dc drift compensation. In [5], Low-Pass Filters (LPF) with very low cut-off frequency have been proposed to replace the pure integrator, but they introduce phase and gain errors due to their natural delay which causes problems in the frequency range below the filter cut-off frequency [4, 6]. Programmable filters were also proposed to solve this problem by replacing the single stage integrator by cascaded filters with small time constants to attenuate the dc offset decay times. In [7], a three stage programmable cascaded LPF is used for the accurate estimation of the rotor flux. Another technique entirely replaces the voltage model with a state observer with current error feedback which reduces the scheme simplicity [3].

Artificial neural networks have been proposed to model the machine stator flux from present samples of stator voltage and current components [6, 8].

This paper proposes a novel neural network rotor flux observer to replace the conventional voltage model to improve the sensorless drive performance at low speed. The proposed neural network observer shows robustness against stator resistance variation and high noise immunity. It avoids using either a pure integrator or a low pass filter for flux estimation which eliminates integrator drift and initial condition problems.

II. RF-MRAS SPEED OBSERVER

A. Machine Model and Vector Control Strategy

The induction motor mathematical model in d-q coordinates established in a rotor flux oriented reference frame can be written as:

$$v_{sd} = R_S\, i_{sd} + \frac{d}{dt}\psi_{sd} - \omega_e \psi_{sq} \tag{1}$$

$$v_{sq} = R_S\, i_{sq} + \frac{d}{dt}\psi_{sq} + \omega_e \psi_{sd} \tag{2}$$

$$0 = R_r\, i_{rd} + \frac{d}{dt}\psi_{rd} - \omega_{sl}\psi_{rq} \tag{3}$$

$$0 = R_r\, i_{rq} + \frac{d}{dt}\psi_{rq} + \omega_{sl}\psi_{rd} \tag{4}$$

where the stator and rotor flux linkages are given by:

$$\psi_{sd} = L_s\, i_{sd} + L_m\, i_{rd} \tag{5}$$

$$\psi_{sq} = L_s\, i_{sq} + L_m\, i_{rq} \tag{6}$$

$$\psi_{rd} = L_m\, i_{sd} + L_r\, i_{rd} \tag{7}$$

$$\psi_{rq} = L_m\, i_{sq} + L_r\, i_{rq} \tag{8}$$

The state space representation of the induction motor with the stator currents and the rotor flux linkages components as state variables can be written as:

$$\begin{bmatrix} \frac{d}{dt}i_{sd} \\ \frac{d}{dt}i_{sq} \\ \frac{d}{dt}\psi_{rd} \\ \frac{d}{dt}\psi_{rq} \end{bmatrix} = \begin{bmatrix} -\left(\frac{R_s}{\sigma L_S} + \frac{1-\sigma}{\sigma T_r}\right) & \omega_e & \frac{L_m}{\sigma L_S L_r T_r} & \frac{L_m \omega_r}{\sigma L_S L_r} \\ -\omega_e & -\left(\frac{R_s}{\sigma L_S} + \frac{1-\sigma}{\sigma T_r}\right) & -\frac{L_m \omega_r}{\sigma L_S L_r} & \frac{L_m}{\sigma L_S L_r T_r} \\ \frac{L_m}{T_r} & 0 & -\frac{1}{T_r} & (\omega_e - \omega_r) \\ 0 & \frac{L_m}{T_r} & -(\omega_e - \omega_r) & -\frac{1}{T_r} \end{bmatrix} \begin{bmatrix} i_{sd} \\ i_{sq} \\ \psi_{rd} \\ \psi_{rq} \end{bmatrix} + \begin{bmatrix} \frac{1}{\sigma L_S} & 0 \\ 0 & \frac{1}{\sigma L_S} \\ 0 & 0 \\ 0 & 0 \end{bmatrix} \begin{bmatrix} v_{sd} \\ v_{sq} \end{bmatrix} \tag{9}$$

where T_r is the rotor time constant and is given by:

$$T_r = \frac{L_r}{R_r} \tag{10}$$

and σ is the leakage coefficient given by:

$$\sigma = 1 - \frac{L_m^2}{L_s L_r} \tag{11}$$

The electromagnetic torque and the rotor speed are given by:

$$T_{em} = \frac{3}{2} P \frac{L_m}{L_r}\left(i_{sq}\psi_{rd} - i_{sd}\psi_{rq}\right) \tag{12}$$

$$\frac{d\omega_r}{dt} = \frac{P}{J} T_{em} - \frac{B}{J}\omega_r - \frac{P}{J} T_l \tag{13}$$

where:

R_s and R_r are the stator and rotor winding resistances;

L_s, L_m and L_r are the stator, mutual and rotor inductances;

P is the number of pole pairs;

ω_e , ω_r and ω_{sl} are the synchronous, rotor and slip speed in electrical rad/s;

v_{sd} , v_{sq} , i_{sd} , i_{sq} , ψ_{rd} and ψ_{rq} are stator voltage, stator current and rotor flux d-q components in the rotor flux oriented reference frame;

T_{em} and T_l are the electromagnetic torque and the load torque respectively;

J and B are the motor inertia and viscous friction coefficient respectively

Under the rotor flux orientation conditions the rotor flux is aligned on the d-axis of the d-q rotor flux oriented frame and the rotor flux equations can be written as:

$$\psi_{rq} = 0 \tag{14}$$

$$\psi_{rd} = L_m i_{sd} \tag{15}$$

The slip frequency can be calculated from the reference values of the stator current components represented in the rotor flux oriented reference frame as follow [4]:

$$\omega_{sl} = \omega_e - \omega_r = \frac{1}{T_r}\frac{i_{sq}^*}{i_{sd}^*} \tag{16}$$

and the electromagnetic torque equation can be written as:

$$T_{em} = \frac{3}{2} P \frac{L_m}{L_r}\psi_r\, i_{sq} = K_t\, i_{sq} \tag{17}$$

where K_t is the torque constant given by:

$$K_t = \frac{3}{2} P \frac{L_m}{L_r}\psi_r \tag{18}$$

In Indirect Rotor Field Oriented Control (IRFOC), the rotor flux position (θ_e) is given by:

$$\theta_e = \int \omega_e dt = \int (\omega_{sl} + \omega_r) dt = \int \left(\frac{1}{T_r}\frac{i_{sq}^*}{i_{sd}^*} + \omega_r\right) dt \tag{19}$$

The block diagram of a sensorless indirect rotor field oriented control induction motor drive is shown in Fig.1. Based on terminal voltages and currents, the observer estimates the motor speed and the rotor flux vector. Estimated motor speed is used to calculate the rotor flux position (θ_e) as in (19) as well as in the speed control loop whereas the estimated rotor flux can be used in the flux control loop or to estimate the flux position in Direct Rotor Field Oriented Control scheme (DRFOC).

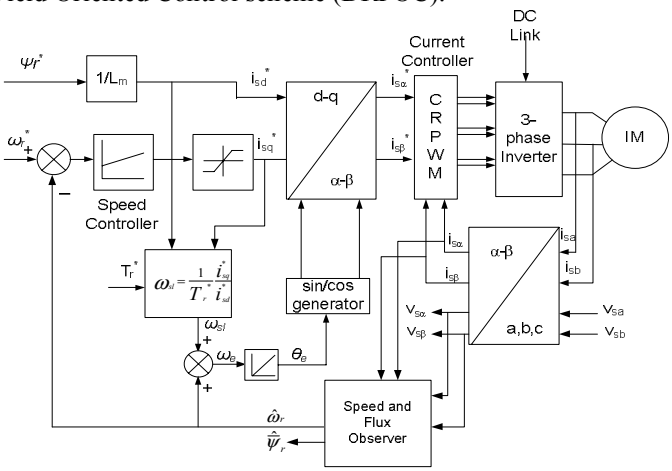

Fig.1 Sensorless indirect vector control

B. RF-MRAS speed observer

The basic concept of MRAS is the presence of a reference model which determines the desired states and an adaptive (adjustable) model which generates the estimated values of the states. The error between these states is fed to an adaptation mechanism to generate an estimated value of the rotor speed which is used to adjust the adaptive model. This process continues till the error between two outputs tends to zero [3, 4]. Basic equations of rotor flux based-MRAS can be written as:

$$\dot{\boldsymbol{\psi}}_{\mathbf{r}} = \frac{L_r}{L_m}\{\mathbf{v_s} - R_s \mathbf{i_s} - \sigma L_s \dot{\mathbf{i}}_{\mathbf{s}}\} \tag{20}$$

$$\dot{\hat{\boldsymbol{\psi}}}_{\mathbf{r}} = \left(-\frac{1}{T_r} + j\hat{\omega}_r\right)\hat{\boldsymbol{\psi}}_{\mathbf{r}} + \frac{L_m}{T_r}\mathbf{i_s} \tag{21}$$

The reference model (20) is based on stator equations and is therefore independent of the motor speed, while the adaptive model (21) is speed-dependant since it is derived from the rotor equation in the stationary reference frame. To obtain a stable nonlinear feedback system, a speed tuning signal (ε_ω) and a PI controller are used in the adaptation mechanism to generate the estimated speed. The speed tuning signal and the estimated speed expressions can be written as [4]:

$$\varepsilon_\omega = \mathrm{Im}\left(\boldsymbol{\psi}_r \hat{\boldsymbol{\psi}}_r^*\right) = \psi_{rq}\hat{\psi}_{rd} - \psi_{rd}\hat{\psi}_{rq} \tag{22}$$

$$\hat{\omega}_r = \left\{k_p + \frac{k_i}{s}\right\}\varepsilon_\omega \tag{23}$$

where "*" denotes complex conjugate.

The block diagram of a RF-MRAS speed observer is shown in Fig.2. The adaptive model represented by (21) can be replaced by a two layer linear neural network. The application of this strategy avoids using mathematical model employing pure integration and the adaptation mechanism is integrated into the network tuning law which reduces the problem of tuning the PI controller gains [5]. However, in this paper a conventional current model (21) will be used as the adaptive model.

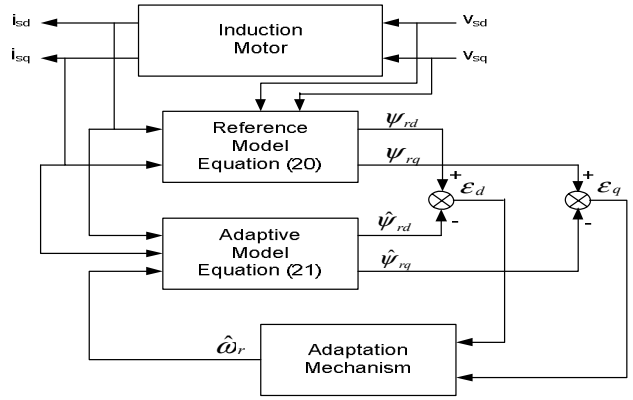

Fig.2 RF-MRAS speed observer

Generally the RF-MRAS observer gives satisfactory speed estimation in the high and medium speed regions. When working at low speed the observer performance deteriorates due to the stator resistance mismatch, integrator drift and initial condition problems and sensitivity to current measurement noise. Therefore an artificial neural network is proposed to replace the conventional voltage model flux observer (20) to improve the MRAS scheme performance at low speed.

III. NEURAL NETWORK FLUX OBSERVER

A. *Artificial Neural Networks*

Artificial Neural Networks (ANN) are based on the basic model of the human brain with the capability of generalization and learning. They can be used as universal function approximators to represent functions with weighted sums of nonlinear terms [8]. This is useful when representing some systems which do not have an accurate mathematical model. It has been shown that any nonlinear function can be represented by a three layer neural network, i.e. input, hidden and output layers, with a given number of neurons in each layer and that the accuracy of the approximation depends on the number of neurons in the hidden layer [9]. The unit of structure of ANN is the neuron which consists of a summer and an activation function as shown in Fig. 3. The commonest type of ANN is the multi-layer feedforward neural network which consists of layers; each layer consists of neurons as shown in Fig. 4 [5].

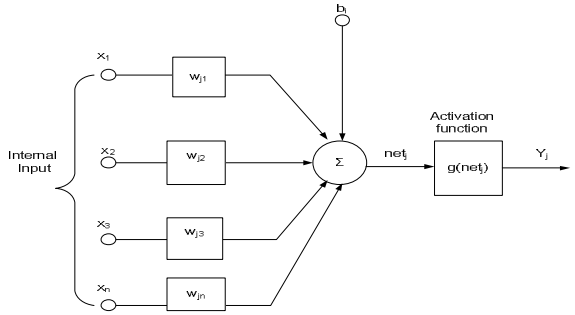

Fig.3 Structure of the artificial neuron

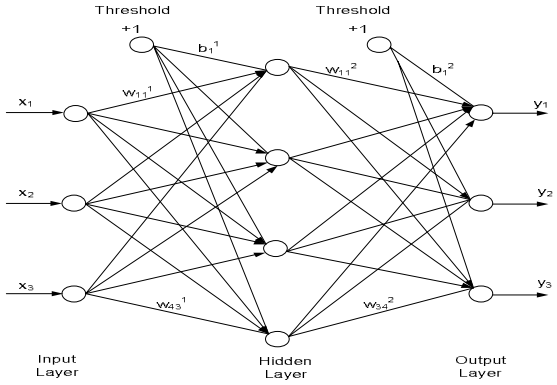

Fig.4 Architecture of multi layer feedforward neural network

Consider a neuron j in a layer m with n inputs in the (m-1) layer and a threshold (b). The net input to the neuron is given by:

$$net_j = \sum_{k=1}^{n} w_{jk}x_k + b_j = w_{j1}x_1 + w_{j2}x_2 + \ldots + w_{jn}x_n + b_j \tag{24}$$

and the neuron output is given by:

$$y_j = g\left(net_j\right) = g\left\{\sum_{k=1}^{n} w_{jk}\, x_k + b_j\right\} \tag{25}$$

where (g) is the activation function or the neuron transfer function. The commonest activation functions are: threshold, linear, logsigmoid and tansigmoid activation [9]. In this paper, tansigmoid activation will be used and in this case, the neuron transfer function can be written as:

$$y_j = \tanh(net_j) = \frac{1 - \exp(-net_j)}{1 + \exp(-net_j)} \tag{26}$$

B. Artificial Neural Network rotor flux observer

In this type of learning a set of input/ target data is used to train the neural network. This is called supervised learning due to the availability of a teacher in the form of target values [5]. At each time the neural network output is compared with the target value and a weight correction via a learning algorithm is performed in such a way to minimize the error between the two values. This is an optimization problem in which the learning algorithm is searching for the optimal weights that can represent the solution to the approximation problem. A lot of techniques have been proposed as learning algorithms such as: back propagation algorithm, Kalman Filter, least square method, etc. A block diagram of the training process is shown in Fig. 5 [6].

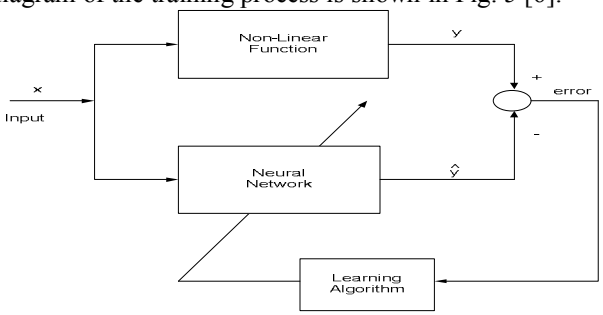

Fig.5 Neural Network in training phase

To estimate the rotor flux components in the stationary reference frame an 8-20-2 multilayer feedforward neural network is proposed as shown in Fig. 6. To obtain good estimation accuracy, the inputs to the network are the present and past values of the d-q components of the stator voltage and current in the stationary reference frame. This is different from [6, 8] which uses only the present samples. Since the inverter is current controlled, the filtered stator voltage is used instead of the inverter PWM voltage due to the unavailability of reference stator voltages as in the case of a voltage controlled inverter. Better performance can be obtained by increasing the number of inputs to include voltage and current samples from more than one time step in the past. However, this may require larger training data and will need more computational effort to achieve good approximation accuracy. The number of neurons in the hidden layer is chosen by a trial error technique to compromise between computational complexity if a larger number is selected and approximation accuracy if a smaller number is selected. The output layer consists of two neurons representing the rotor flux components in the stationary reference frame. Since the case is approximating a nonlinear function, tansigmoid activation functions will be used in both hidden and output layers. To generate the training data, the vector controlled induction motor running at different speed commands in the low speed region and subjected to various load torques is simulated and the input/output training pattern is obtained with a sampling frequency of 2 kHz. 4800 samples in the low speed region were obtained and are used to train the network. The training is performed off-line using the Levenberg-Marquardt algorithm which is faster than the gradient descent back propagation algorithm. After the training the Mean Squared Error (MSE) between targets and neural network outputs decays to 6 10^{-5} after 900 epochs as shown in Fig. 7.

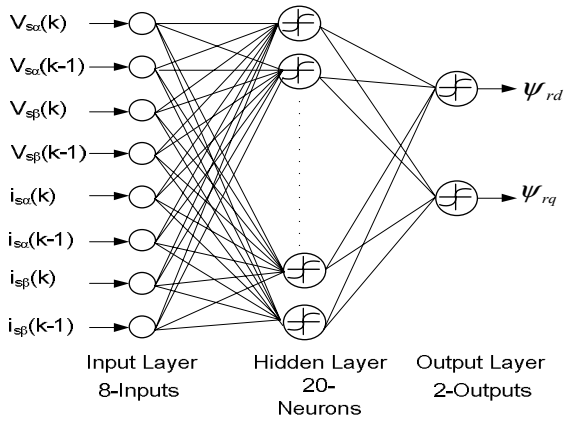

Fig.6 Neural Network rotor flux observer

To improve the speed estimation performance of RF-MRAS at low speed, the trained neural network is proposed to replace the conventional voltage model (20) to benefit from its advantages such as: fault tolerance, noise immunity and fast processing speed and in this case the estimated speed is obtained through a low pass filter.

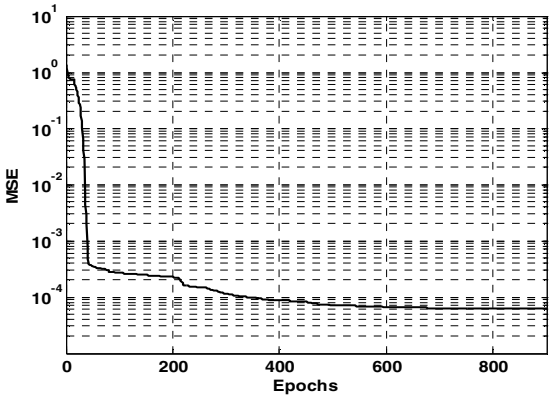

Fig.7 NN performance during training

IV. SIMULATION RESULTS AND DISCUSSION

To study the performance of the RF-MRAS speed observer, an induction motor vector control drive shown in Fig.1 is simulated using Matlab-Simulink when running at low speed region. Induction motor parameters are given in table I. Two RF-MRAS schemes will be compared: the first scheme uses the conventional voltage model (20) as a reference model whereas the other scheme makes use of the NN rotor flux observer discussed in section III instead. During the simulation, the sampling frequency of the NN flux observer is 1 kHz. The drive is running under variable speed commands of 20, 30 and 40 electrical rad/s applied each 0.6s. At each speed command, the motor is running at no load for 0.3 s and then is loaded with its rated load torque for 0.3s. These speed commands are already seen by the NN observer during training. The stator resistance (R_s) is set equal to its nominal value in the first 0.6s. At t=0.6s and 1.2s a 5% and 10% step increase in the actual R_s is applied respectively. The stator resistance value used in the

conventional MRAS scheme is set equal to the nominal value during the simulation. To study the effect of noise on the observer performance, white noise with power of 10^{-5} is added to the stator current measurement in both schemes. The flux estimation using both techniques is shown in Fig. 8; the flux estimated with conventional voltage model is mismatching the real machine flux when R_s variation occurs whereas NN flux observer is still tracking the real flux even in the presence of R_s variation. Consequently, the estimated speed obtained from NN-MRAS is more accurate compared to that obtained from conventional MRAS as shown in Fig. 9 due to the fault tolerance and noise immunity features of neural networks. However the estimated speed using the NN scheme contains some ripples which depend upon the sampling time used in the NN observer to approximate the rotor flux. Decreasing this sampling time may need a lot of training data [8].

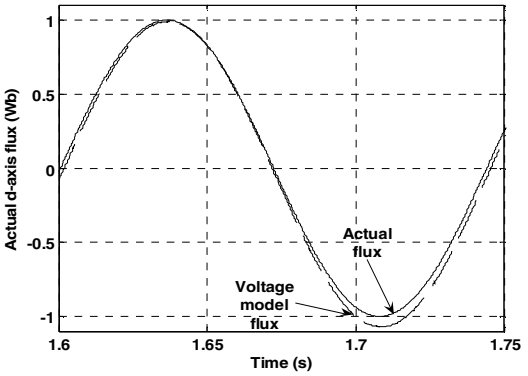

(a)

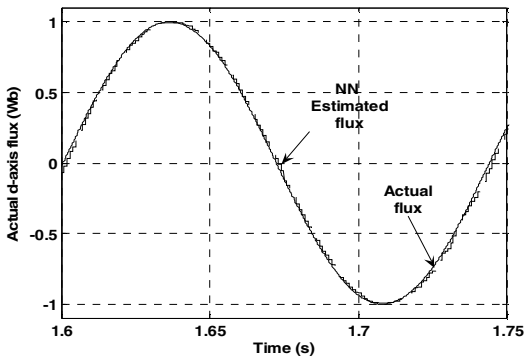

(b)

Fig.8 Rotor flux estimation (a) Voltage model (b) NN model

To test the generalization property of the neural network observer, the drive was run at different speed commands of 20, 35 and 45 rad/s with the same conditions as the first case. The last two speeds were not seen during the training of the NN flux observer; 35 rad/s is inside the training range while as 45 rad/s is outside the training range. Due to the complete tracking of the actual flux achieved by the NN observer, satisfactory speed estimation is still obtained by the NN-MRAS scheme even in the presence of R_s variation and current measurement noise compared to the conventional scheme as shown in Fig.10. However, the speed estimation at 35 rad/s is more accurate than that at 45 rad/s which proves that neural networks have better generalization property for the points which are within the training range compared to those which are out of the training range.

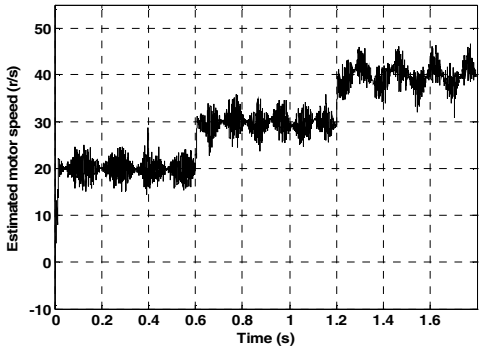

(a)

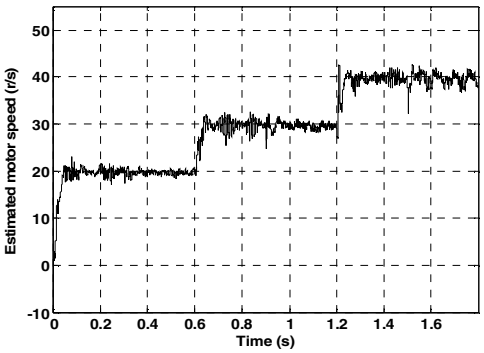

(b)

Fig.9 Motor speed estimation (a) MRAS (b) NN-MRAS

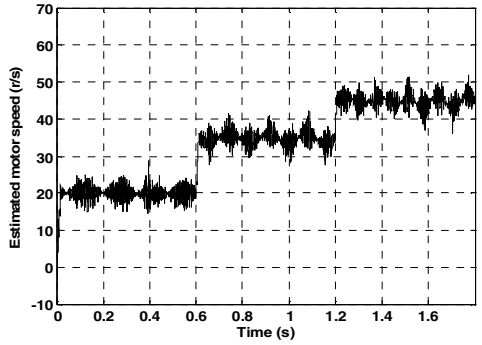

(a)

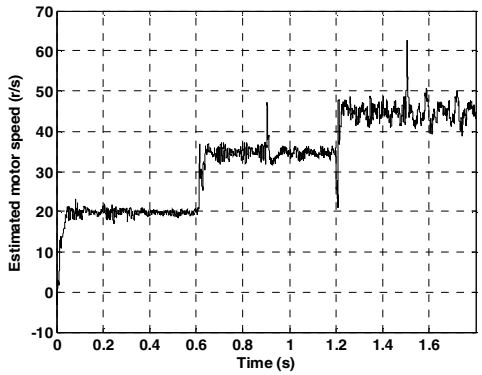

(b)

Fig.10 Motor speed estimation (a) MRAS (b) NN-MRAS

Finally, if a 1% mismatch in the initial condition of the integrator occurs, a drift occurs in the estimated speed which is not the case with the NN due to the presence of bounded tansigmoid (hyperbolic tangent) activation function in the hidden and the output layers [8]. The estimated speeds obtained by the two schemes are shown in Fig. 11.

The simulation results of the conventional MRAS observer are obtained using pure integration. However, if a low pass filter is used instead in both reference and adaptive models, the observer performance will be even worse especially at low speed below the cutoff frequency, which is not the case with the proposed hybrid MRAS-NN scheme which does not employ either pure integration or a low pass filter.

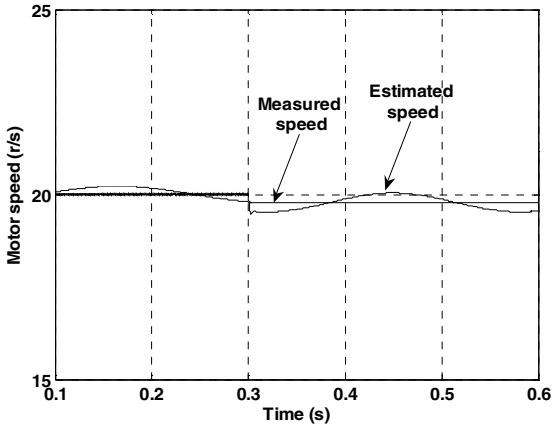

(a)

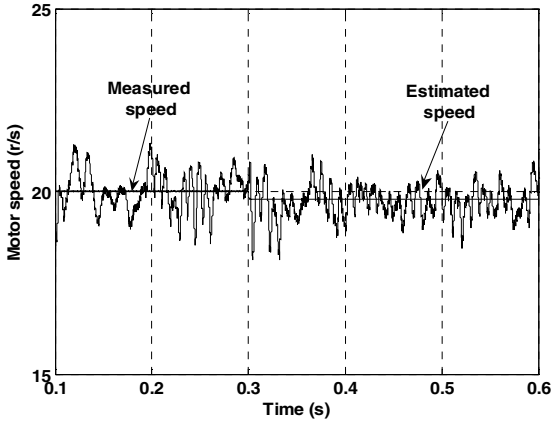

(b)

Fig.11 Motor speed estimation (a) MRAS (b) NN-MRAS

TABLE I
Induction motor parameters

Machine parameter	Value	Machine parameter	Value
Rated Power	7.5 [kW]	R_r	0.24892 [Ω]
Rated Voltage	415 / 239 [V]	L_s	106.37 [mH]
Rated Speed	309.8 [elec rad/s]	L_m	101.467 [mH]
Rated Torque	48.39 [N.m]	L_r	106.37 [mH]
Rated frequency	50 [Hz]	J	0.15 [Kg/m^2]
R_s	0.7866 [Ω]	Pole number	4

V. CONCLUSION

In this paper an ANN is presented as a rotor flux observer to replace the conventional voltage model used in RF-MRAS speed observer when working at low speed. Results show that the NN model improves the MRAS observer performance at low speed operation compared with the conventional voltage model when stator resistance mismatch, measurement noise and drift problems take place. Moreover, no stator resistance adaptation scheme is required. Accurate rotor flux estimation is obtained using the neural network observer which can be used for flux control in the vector control drive. The presented scheme still needs improvement to reduce the ripples of the estimated speed around the actual speed.

REFERENCES

[1] J. Holtz and J. Quan, "Drift and parameter compensated flux estimator for persistent zero stator frequency operation of sensorless controlled induction motors," *IEEE Trans. Industry Applications*, vol. 39, no. 4, July/August 2003, pp.1052-1060.

[2] M. Rashed and A.F. Stronach, "A stable back-EMF MRAS-based sensorless low speed induction motor drive insensitive to stator resistance variation," *IEE Proc. Electr. Power Appl.*, vol. 151, no. 6, November 2004, pp. 685-693.

[3] Y.A. Kwon and D. Won Jin, "A novel MRAS based speed sensorless control of induction motor," in *Proceedings of the 25th Annual Conf. of the IEEE Industrial Electronics Society, IECON'99*, vol. 2, pp. 933-938.

[4] P. Vas, *Sensorless Vector and Direct torque control*, Oxford University Press, New York, 1998.

[5] L. Ben-Brahim, S. Tadakuma and A. Akdag, "Speed control of induction motor without rotational transducers," *IEEE Trans. Industry Applications,* vol. 35, no. 4, July/August 1999. pp. 844-850.

[6] Y. Yusof and A.H.M. Yatim, "Simulation and modelling of stator flux estimator for induction motor using artificial neural network technique," in *Proceedings of National Power and Energy Conf. (PECon)*, 2003, pp.11-15.

[7] B. Karanayil, M.F. Rahman and C. Grantham, "An implementation of a programmable cascaded low-pass filter for a rotor flux synthesizer for an induction motor drive," *IEEE Trans. on Power Electron.,* vol. 19, no. 2, March 2004. pp. 257-263.

[8] L.M. Grzesiak and B. Ufnalski, "Neural stator flux estimator with dynamical signal preprocessing," in *Proceedings of the IEEE AFRICON*, 2004, pp. 1137-1142.

[9] H. Lu, T. Hung and C. Tsai, "Sensorless vector control of induction motor using artificial neural network," in *Proceedings of IEEE International Symposium on Circuits and Systems (ISCAS 2000)*, pp. 489-492.